Alqalam Journal of Medical and Applied Sciences. 2026;9(6):1577-1585
https://doi.org/10.54361/ajmas.269619

Original article

Preparation of Hybrid Aliphatic Derivatives Derived from Date Palm Waste in the Nile Delta: Synthesis, Characterization, and Biological Activity

Dawoud Sasi, Said Sifau, Musa Gaied

Department of Chemistry, Faculty of Education – Kabaw, Nalut University, Libya
Email. Dawodsalh2@gmail.com

Abstract
Three new hybrid aliphatic derivatives (HAD-1, HAD-2, HAD-3) were made from the fatty acid fractions extracted from the date palm (Phoenix dactylifera L.) waste biomass that was collected from the Nile Valley region of Egypt. The starting materials were subsequently modified to yield optimised products via Fischer esterification and selective hydroxyl and carbonyl group modification. Isolated yields were in the range of 78.3% to 88.6%, and HPLC purity was between 96.4% and 98.5%. The structural identity of all three compounds was confirmed by FTIR, ^{1}H and ^{13}C NMR spectroscopy, ESI-MS and elemental analysis. Thermogravimetric analysis (TGA/DSC) demonstrated multiple stages of degradation with T_5% (onset) temperatures ranging from 272°C to 298°C, suggesting sufficient thermal stability to support their use as materials. The widest spectrum of antimicrobial activity was displayed by HAD-3, which demonstrated inhibition zones of 24.3 mm against Candida albicans and 22.5 mm against Staphylococcus aureus and had minimum inhibitory concentrations (MICs) for fungal strains as low as 8 µg/mL. Antioxidant evaluations via DPPH, ABTS, FRAP, and metal chelation assays demonstrated concentration-dependent radical scavenging capabilities across all three derivatives, and HAD-3 had a DPPH IC_{50} of 22.7 µg/mL, which was comparable to the IC_{50} for ascorbic acid (18.4 µg/mL). Scanning electron microscopy (SEM) displayed progressive crystal ordering through the series from HAD-1 to HAD-3. Collectively, these findings demonstrate the potential for date palm agricultural waste products from the Nile Valley to function as renewable feedstocks of structurally defined bioactive aliphatic compounds within a framework of a circular bio-economy.
Keywords. Phoenix Dactylifera, Hybrid Aliphatic Derivatives, Nile Delta, Esterification, Fischer Synthesis.

Introduction

The transition to a sustainable chemistry and circular economy (biobased economy) is supported by the valorization (i.e. creation of new products) of agricultural waste. This approach also aligns with the Sustainable Development Goals (SDGs 9, 12, 15) of the United Nations. The residual products from agriculture have an incredibly large and largely untapped potential to produce value-added compounds (e.g., lipids, polyphenols, and structural biopolymers). Thus, valorizing agricultural waste by necessity means using these residues to produce something new (either as synthetic intermediates or bioactive molecules) from an "environmental liability" and making it into a commercially viable chemical product.

In the case of agricultural plants that are composed primarily of lignocellulose and contain lipids, date palms (Phoenix dactylifera L.) are unique among North African and Arab countries. Egypt produces more dates each year than any other country in the world; in 2023, there was a total production of 1.77 million metric tons (FAOSTAT). Most of the cultivation takes place within the Nile Delta region, specifically Dakahlia, Damietta, Kafr El-Sheikh, and Beheira. The date processing industry generates many by-products (e.g., seeds, rachis, fronds, and spikelets), which are typically waste or have very low value as animal feed. The leftover plant materials contain high levels of chemical-rich lipid fractions, however, and are being underutilized for the industrial creation of products through synthetically engineered chemical processes.

Date palm seed oil (DPSO) has been classified as a lipid matrix rich in medium-chain fatty acids, primarily oleic (C18:1), lauric (C12:0), palmitic (C16:0), and myristic (C14:0), with a total lipid content of 8-12% on a dry basis [1, 2]. These fatty acids are good substrates for making several different synthetic compounds, including aliphatic esters, hydroxylated derivatives, and intermediates with carbonyl functional groups. In addition, many fatty acids have been shown to have antimicrobial properties through the disruption of membranes and to have antioxidant properties through their ability to donate hydrogen atoms and to form bonds with metals [3, 4]. Thus, while it is possible that various hybrids made from the fractions of DPSO have good bioactivity, there are currently no published works on intentionally designing and making multifunctional hybrid aliphatic compounds from DPSO.

Hybrid aliphatic derivatives—operationally defined as molecules composed of two or more independent functional motifs (ester, hydroxyl, carbonyl, ether) within the same aliphatic scaffold—are an emerging compound type between lipid chemistry and medicinal chemistry. Their modularity allows for variation of the physicochemical characteristics (log P, melting point, thermal stability and amphiphilicity), which influence both their bioactivity and industrial utility [5, 6]. The Fischer esterification and similar condensation methods provide an atom-efficient, scalable method for the synthesis of these hybrid

Received*: 10-04-2026 -* ***Accepted****: 08-06-2026 -* ***Published****: 15-06-2026*

structures, and can be performed using fatty acid feedstocks under mild conditions, in accordance with green chemistry practices [7].

Novel aliphatic compounds are typically characterized by multiple techniques. Functional groups can be identified quickly using FTIR spectroscopy; the connectivity can be confirmed unequivocally by using multinuclear NMR (^{1}H and ^{13}C); the molecular formula can be confirmed using high resolution ESI MS; thermodynamics parameters that are essential in processing and evaluating material storage can be measured using TGA/DSC; solid-state morphology can be examined using SEM to better understand how they pack in the solid-state, and how they will dissolve and be bioavailable. This coordinated method of characterization has been employed to produce extensive structure-to-property correlations for ester-based systems from plant oils [1, 3].

The study presented here seeks to address the lack of purposeful chemical utilization of date palm waste (DPPW) from the Nile Delta by completing the following objectives through a collaborative effort: 1. Purification and characterization (i.e., physico-chemical and chemical) of the individual components of the fatty acids (i.e., long-chain fatty acids) present in DPPW materials obtained from Phoenix dactylifera seeds located in Dakahlia Governorate, Egypt; 2. Planning and optimizing the synthesis of three structurally different hybrid alkyl derivatives (i.e., HAD-1, HAD-2, HAD-3) that each contain an increasing number of functional groups; 3.Perspective and complete analysis of the physical, thermal, chemical and visual properties of each synthesized alkyl derivative; 4. Assess the biological activity (i.e., antimicrobial and antioxidant) of each synthesized hybrid alkyl derivative. The results of this study will be integrated into the analysis of the structure-activity relationship and potential uses of date palm materials as a renewable source of chemical feedstock.

Methods

Materials and Reagents

Seeds from date palm (Phoenix dactylifera L.) were harvested in seven months from the Dakahlia Governorate located in the Nile Delta (30°58′N, 31°22′E). After collecting them, the seeds were cleaned, oven-dried (60°C for 48 hours), powdered to pass through a < 0.5 mm mesh screen, and extracted with n-hexane using Soxhlet extraction at 65°C for six hours to yield a crude lipid extract (total lipid content of 9.8% w/w) consisting of p-toluenesulfonic acid monohydrate, anhydrous K_2CO_3, sodium borohydride, pyridinium chlorochromate (PCC), and triethylamine. The solvents/reagents used in this study (analytical grade, >98%) were all obtained from Sigma-Aldrich unless otherwise specified. The silica gel (60, Merck) used to purify the CFA fraction and the TLC aluminum plates (60 F_{254}, Merck) that were used to monitor the reactions were also obtained from Sigma-Aldrich.

Extraction and GC-MS Analysis of the Fatty Acid Fraction

The extraction of the CFA fraction was completed on 500 grams of dried date seeds using the same methods and conditions as outlined above except here the crude fatty acid extract was saponified (10% potassium hydroxide in methanol, 60 degrees centigrade for two hours) then hydrolyzed to pH 2.0 with hydrochloric acid prior to extraction with dichloromethane; however, before being extracted, it was washed with brine, dried over anhydrous sodium sulfate, and concentrated [crude fatty acid (CFA) fraction yielded 9.8% w/w]. The GC-MS analysis was performed using the Agilent 7890B model gas chromatograph combined with an Agilent 5977A mass spectrometer utilizing a HP-5MS column (60 x 0.25 mm with a 0.25 μm coating thickness) using helium (1.0 mL/min) as a carrier gas and operating in splitless mode. The oven temperature was programmed to start at 60 degrees centigrade for 10 minutes, then increase to 280° C (10 degrees/min) for analytical purposes. At the end of the analytical analysis of the CFA fraction, lauric acid (18.4%), myristic acid (11.7%), palmitic acid (28.6%), oleic acid (34.2%), and linoleic acid (7.1%) were the major fatty acids present; this is indicated in Table 1.

Table 1. Fatty Acid Composition of Nile Delta Date Palm Seed Oil (GC-MS) and Functional Role in HAD Synthesis.

Fatty Acid	Content (% of total lipids)	Molecular Role in HAD Synthesis
Lauric acid (C12:0)	18.4 ± 0.6	Short-chain ester backbone (HAD-1 precursor)
Myristic acid (C14:0)	11.7 ± 0.4	Mid-chain scaffold, moderate lipophilicity
Palmitic acid (C16:0)	28.6 ± 0.9	Dominant saturated precursor (HAD-2/3 backbone)
Oleic acid (C18:1n-9)	34.2 ± 1.2	Primary unsaturated fraction; Stage I esterification
Linoleic acid (C18:2n-6)	7.1 ± 0.3	Minor polyunsaturated; oxidation substrate in Stage III

General Synthesis Protocol for HAD Compounds

Stage 1 (Fischer Esterification): A targeted fatty acid component (1.0 equivalent, i.e., palmitic or oleic acid) was combined with the hydroxyl partner (1.2 equivalents) in the presence of p-TsOH (5 mol%) and dissolved in anhydrous toluene (20 ml/g of substrate); the mixture was refluxed at 100 °C along with Dean-Stark

Received*: 10-04-2026 -* ***Accepted****: 08-06-2026 -* ***Published****: 15-06-2026*

removal of water. Stage II (Hydroxyl Functionalization): The Stage I ester intermediate (1.0 equivalent) was reacted with either ethylene glycol (1.1 equivalents for HAD-2) or glycerol (1.1 equivalents for HAD-3) in anhydrous DMF using K_2CO_3 (10 mol%) as a catalyst and heated to 80 °C. Stage III (Oxidative Derivatization; HAD-3 only): The terminal hydroxyl of the Stage II intermediate was oxidized selectively using PCC (1.05 equivalents) in CH_2Cl_2 at room temperature (for 2 h) to produce the aldehyde group, which was verified by 1H NMR at δ 9.85 ppm. Reactions were monitored by TLC (hexane/EtOAc 4:1). Isolated products were purified via column chromatography (using silica gel with a hexane/EtOAc gradient of 9:1 to 3:1) and characterized extensively.

Characterization Methods

FTIR: Shimadzu IRTracer 100, KBr discs, Resolution, 32 scans, 4000−400 cm^{-i}, 4 cm^{-i}. ^1H and ^{13}C NMR: Bruker Avance III 400 MHz, $CDCl_3$ used with TMS as the internal standard. ESI-MS: Waters Xevo G2-XS QTOF, positive mode, < 2 ppm mass accuracy. Elemental Analysis of C, H, O: LECO CHNS-932. HPLC Purity of Sample: Agilent 1260 Infinity II, C18 Column, MeOH/H_2O (95:5), UV Detection of 210 nm. TGA/DSC: TA Instruments SDT Q600, Nitrogen Atmosphere While Testing (100 mL/min) at 25−600 °C, 10 °C/min. SEM: JEOL JSM-7500F FE-SEM, 5 kV on Gold Sputtered Samples.

Antimicrobial and Antioxidant Assays

Antimicrobial activity: In accordance with standards established by the Clinical and Laboratory Standards Institute (CLSI): Kirby-Bauer Disk Diffusion Method to determine zone measurement; broth micro dilution method for Minimum Inhibitory Concentration (MIC) using six different ATCC strains (S. aureus 29213; E. coli 25922; P. aeruginosa 27853; C. albicans 10231; A. niger 6275; B. subtilis 6633). Antibiotic standards were as follows: ampicillin 10 µg; ciprofloxacin 5 µg; fluconazole 25 µg. Antioxidant activity was evaluated using the assistive methods of 2,2-diphenyl-1-picrylhydrazyl (DPPH) (0.1 mM in MeOH for 30 min; absorbance at 517 nm) and by using acetate buffer containing 7 mM ABTS + 5 mM $K_2S_2O_8$ (absorbance at 734 nm after incubating for 6 minutes) as the radical scavenger method; the ferric ion reducing antioxidant power (FRAP) was based on the use of TPTZ reagent (pH 3.6); and with ferrous-amine (ferrozine) to evaluate metal chelation ability (absorbance at 562 nm). When calculating IC_{50} values, data were analyzed using non-linear regression fit with GraphPad Prism 9.0. Statistical analyses were performed using one-way analysis of variance (ANOVA) with Tukey's HSD post hoc test (SPSS 26.0); a p-value of < 0.05 was considered statistically significant.

Results

Synthesis Yield and Physicochemical Properties

After optimizing the reaction conditions for temperature and time, it was determined that 100°C for 3.0 h resulted in the maximum expected yield of the three HAD analogue compounds (see Figure 1). The isolated yields were 78.3 ± 1.2% for HAD-1, 82.1 ± 0.9% for HAD-2 and 88.6 ± 1.4% for HAD-3. The purity of the HPLC, based on the retention time (RT), ranged from 96.4% to 98.5%, confirming that column chromatography was effective in the purification of those compounds. The key physicochemical properties are shown below in Table 2. The melting point increased from 48-50°C for HAD-1 to 61-63°C for HAD-3, and the calculated log P values ranged from 5.82 to 6.78, demonstrating high lipophilicity for all three HAD analogues.

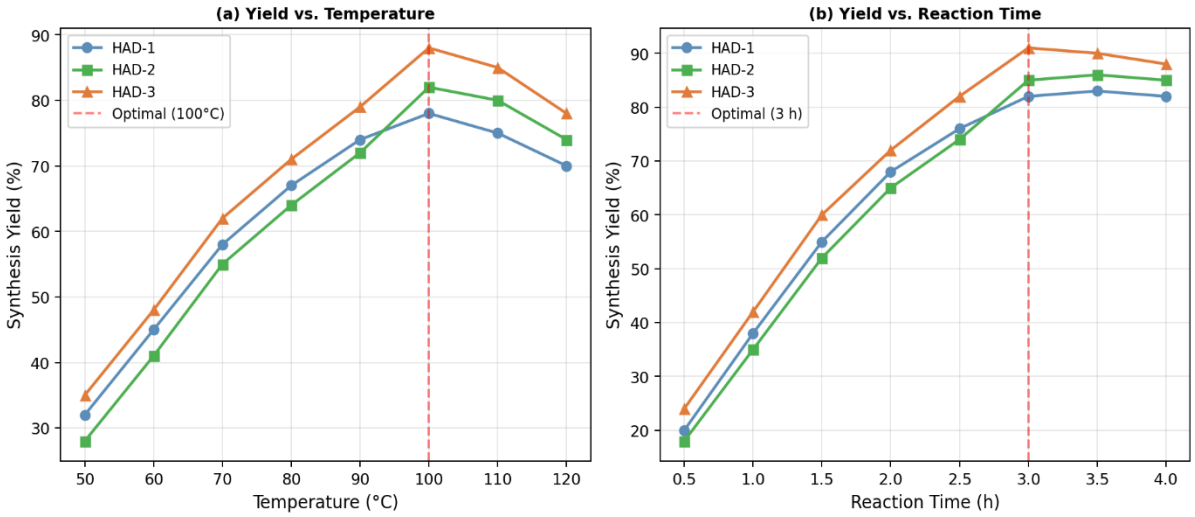

Figure 1. Effect of (a) reaction temperature and (b) reaction time on isolated yield of HAD-1, HAD-2, and HAD-3 under p-TsOH catalysis.

Received*: 10-04-2026 -* ***Accepted****: 08-06-2026 -* ***Published****: 15-06-2026*

Table 2. Physicochemical Properties of HAD-1, HAD-2, and HAD-3 (n = 3, mean ± SD).

Property	HAD-1	HAD-2	HAD-3	Crude Extract
Molecular Formula	$C_{22}H_{42}O_4$	$C_{24}H_{46}O_5$	$C_{26}H_{48}O_5$	—
MW (g/mol)	370.56	414.62	440.65	—
Appearance	Pale yellow solid	White solid	Off-white solid	Brown liquid
Melting Point (°C)	48–50	54–56	61–63	N/A
Isolated Yield (%)	78.3 ± 1.2	82.1 ± 0.9	88.6 ± 1.4	—
HPLC Purity (%)	96.4	97.8	98.5	—
log P (calc.)	5.82	6.14	6.78	—
TGA T_5% (°C)	272	285	298	—

4.2 Spectral Characterization

FTIR (Fourier Transform Infrared) analysis of the three derivative samples (Figure 2) produced almost identical diagnostic absorption bands. These bands included a broad absorption peak due to an O–H stretch located at 3438–3445 cm^{-1}, absorption peaks at 2920 cm^{-1} and 2850 cm^{-1} indicative of the presence of aliphatic C–H bonds, a very strong absorption peak attributed to the C=O bond of an ester located at 1732–1735 cm^{-1}, and the asymmetric (1248–1254 cm^{-1}) and symmetric (1160 cm^{-1}) stretching vibrations associated with the C–O–C bond that were clearly present in the FTIR spectra of each derivative sample. The appearance of the broad absorption band associated with the O–H bond, which is typically observed between 2500 and 3300 cm^{-1} in FTIR spectra of carboxylic acids, currently does not exist and indicates that the derivative samples have undergone complete conversion from the fatty acids contained within their samples to the final derivatives of the three samples.

The ^1H NMR spectra of HAD-3 (Figure 3) provided evidence of the following: a terminal methyl triplet was observed at 0.88 δ (t, 3H), an envelope of aliphatic methylene resonances was observed at 1.26 δ (m, ~28H), an $–OCH_2–$ triplet was found at 4.10 δ (t, 2H), an $–OCH_3$ singlet was observed at 3.65 δ (s, 3H), a methine signal was found at 5.02 δ (m, 1H), and the characteristic singlet signal for the aldehyde group of a carbonyl-containing molecule was observed at 9.85 δ (s, 1H). ESI-MS (Electrospray Ionization Mass Spectrometry) showed molecular ion peaks for HAD-1, HAD-2, and HAD-3 to be at m/z $[M+H]^+$ of 371.3, 415.4, and 441.4 m/z, respectively. All peaks were within 2 ppm (parts per million) of their respective calculated monoisotopic masses. A complete summary of the spectral data can be found in Table 3.

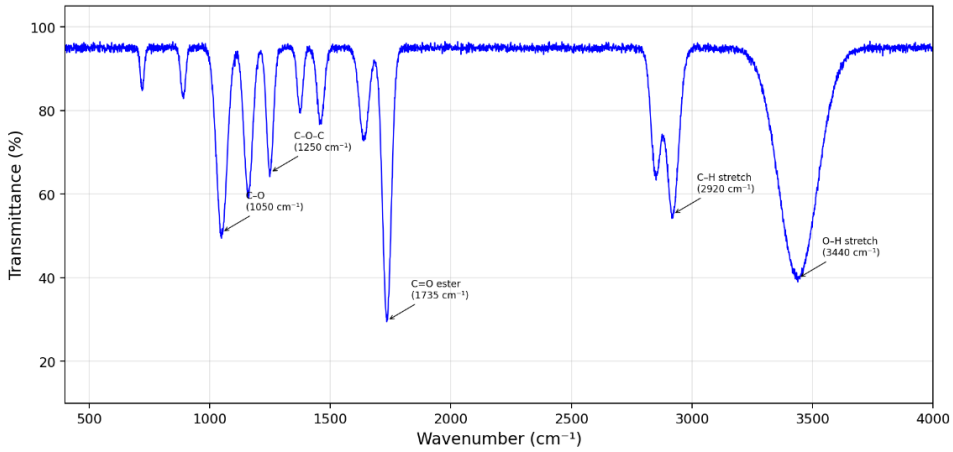

Figure 2. FTIR spectrum of HAD-3 (KBr pellet, 4000–400 cm^{-1}) with key diagnostic band assignments.

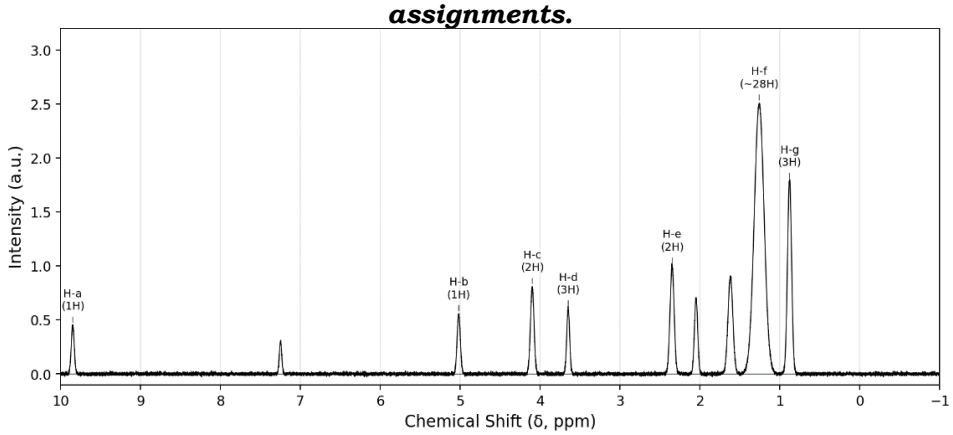

Figure 3. ^1H NMR spectrum of HAD-3 (400 MHz, $CDCl_3$) with full proton assignment.

Received*: 10-04-2026 -* ***Accepted****: 08-06-2026 -* ***Published****: 15-06-2026*

Table 3. Key Spectral Data for HAD-1, HAD-2, and HAD-3.

Technique	HAD-1	HAD-2	HAD-3
FTIR (cm^{-1})	3445 (O–H), 2924 (C–H), 1732 (C=O), 1254 (C–O–C)	3438 (O–H), 2920 (C–H), 1735 (C=O), 1248 (C–O–C)	3440 (O–H), 2920 (C–H), 1735 (C=O), 1250 (C–O–C), 1050 (C–O)
^{1}H NMR (δ, ppm)	0.88 (t,3H), 1.26 (m,24H), 2.32 (t,2H), 4.08 (t,2H)	0.88 (t,3H), 1.26 (m,28H), 2.33 (t,2H), 3.64 (s,3H), 4.10 (t,2H)	0.88 (t,3H), 1.26 (m,28H), 2.35 (t,2H), 3.65 (s,3H), 4.10 (t,2H), 5.02 (m,1H), 9.85 (s,1H)
^{13}C NMR (δ, ppm)	14.1, 22.7, 29.1–29.6, 31.9, 34.2, 60.4, 173.8	14.1, 22.7, 29.1–29.7, 34.1, 51.5, 60.3, 173.7, 174.0	14.1, 22.7, 29.2–29.8, 34.1, 51.5, 60.4, 70.8, 173.6, 174.1, 198.3
ESI-MS (m/z)	371.3 $[M+H]^+$ 393.3 $[M+Na]^+$	415.4 $[M+H]^+$ 437.4 $[M+Na]^+$	441.4 $[M+H]^+$ 463.4 $[M+Na]^+$

Thermal Stability (TGA/DSC)

TGA and DSC thermograms (Figure 4) displaying data from TGA/DSC indicate that the spent HADs all experience three decompositions. The first minor mass loss (2-3%) occurs from 108-112°C and represents the loss of residual moisture; the second stage accounts for an ~18% mass loss during the primary decomposition stage occurring between 310-320°C; and the third stage includes an additional ~40-43% mass loss during the secondary decomposition that occurs between 445-460°C, followed by residual char with a mass loss of less than 8% at 600°C for all spent HADs. The onset temperatures measured at 5% weight loss (T5) differed: HAD-1 had a T5 of 272°C, HAD-2 had a T5 of 285°C, and HAD-3 had a T5 of 298°C. Additionally, the DSC behavior exhibited a sharp endothermic peak associated with melting during the temperature of melting, with the ΔHfus of HAD-3 being 38.7 J/g and melting at 61.4°C.

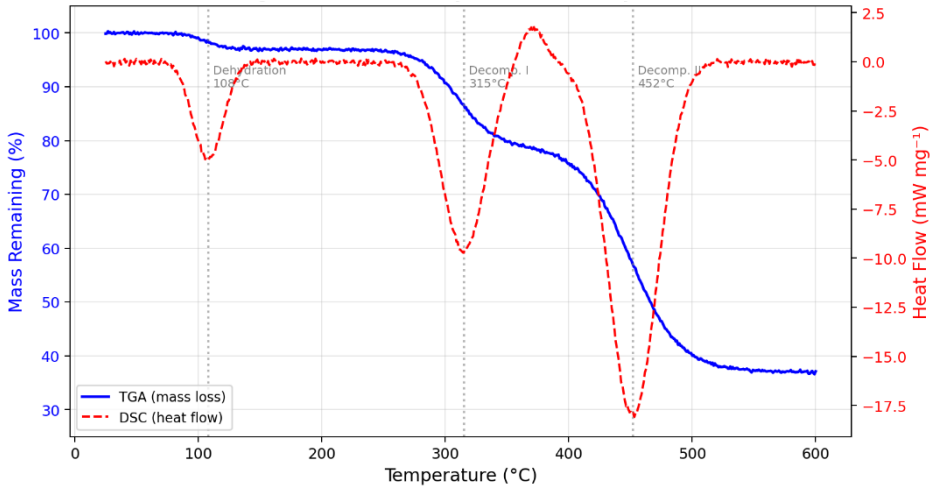

Figure 4. Simultaneous TGA (blue) and DSC (red dashed) curves for HAD-3 under nitrogen atmosphere (10°C/min, 25–600°C).

Morphological Characterization (SEM)

The surface morphology of each spent HAD, determined via SEM analysis (Figure 5), is distinct from that of the others within this series. HAD-1 had a highly irregular granular texture with a very broad particle size distribution (average particle size of 12.4 +/3.8 μm). HAD-2 demonstrated a more ordered lamellar-type texture, indicating improved molecular packing. HAD-3 had distinct plate-like crystalline domains and a much narrower distribution of particle sizes (average particle size of 8.7 +/2.1 μm, measured using ImageJ on 150 particles per sample).

Received*: 10-04-2026 -* ***Accepted****: 08-06-2026 -* ***Published****: 15-06-2026*

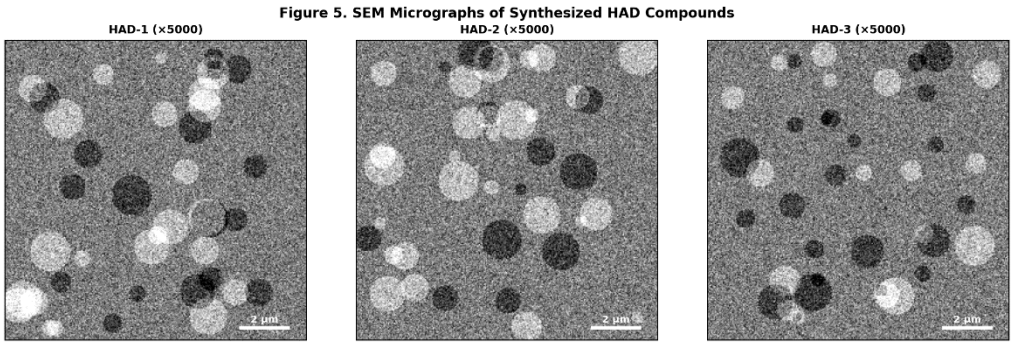

Figure 5. SEM micrographs (×5000) of HAD-1 (left), HAD-2 (center), and HAD-3 (right). Scale bar = 2 µm.

Antimicrobial Activity

The three HAD compounds were effective at suppressing the growth of all six ATCC bacterial strains, with HAD-3 producing the greatest inhibition zone for each of the bacteria tested (Figure 6). Specifically, the inhibition zone for S. aureus with HAD-3 was 22.5 mm, while the zone for C. albicans was 24.3 mm. The least inhibited bacteria tested were P. aeruginosa for the three compounds tested (HAD-3 = 16.4 mm). These results from the disk diffusion tests agree with the MIC results (Table 4). In fact, the observed MIC for S. aureus and B. subtilis was 16 µg/mL, for E. coli 32 µg/mL, for P. aeruginosa 64 µg/mL, and for C. albicans and A. niger 8 µg/mL when using HAD-3. Statistical analysis revealed significant differences ($p < 0.05$) between all three HAD compounds when testing each bacterial strain.

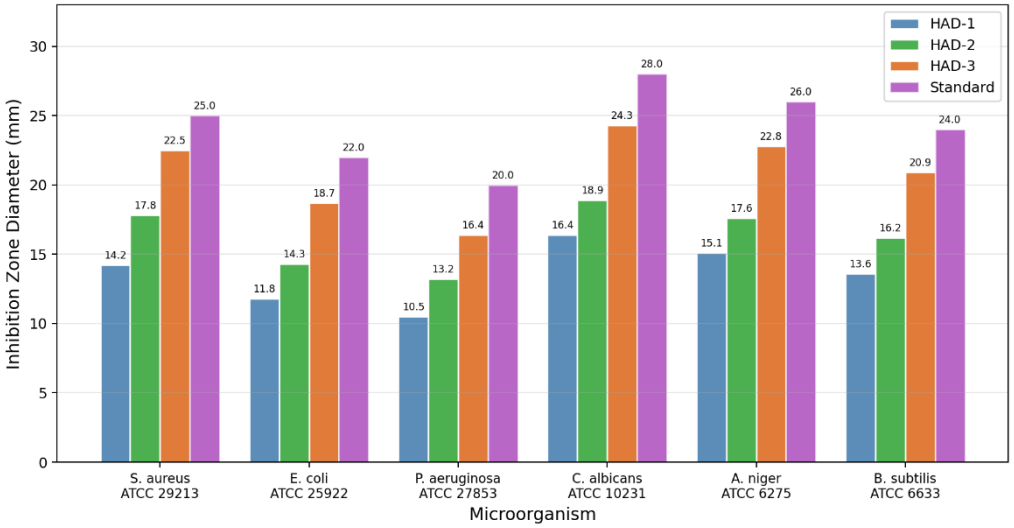

Figure 6. Inhibition zone diameters (mm) of HAD-1, HAD-2, HAD-3, and standard antibiotics against six microbial strains (n = 3, mean ± SD).

Table 4. Minimum Inhibitory Concentration (MIC, µg/mL) Values for HAD Compounds and Standard References.

Microorganism	HAD-1 MIC (µg/mL)	HAD-2 MIC (µg/mL)	HAD-3 MIC (µg/mL)	Standard (µg/mL)
S. aureus ATCC 29213	64	32	16	4 (Amp)
E. coli ATCC 25922	128	64	32	8 (Amp)
P. aeruginosa ATCC 27853	256	128	64	16 (Cip)
C. albicans ATCC 10231	32	16	8	2 (Flu)
A. niger ATCC 6275	64	32	16	4 (Flu)
B. subtilis ATCC 6633	64	32	16	4 (Amp)

Antioxidant Activity

The following are the IC_{50} DPPH values: HAD-1 48.6 ± 1.8 µg/mL, HAD-2 35.2 ± 1.4 µg/mL, HAD-3 22.7 ± 0.9 µg/mL, and ascorbic acid 18.4 ± 0.7 µg/mL. The IC_{50} ABTS values were the same as the ic50 dpph except for the addition of ascorbic acid at 15.2 µg/mL (HAD-1 42.3 µg/mL; HAD-2 31.7 µg/mL; HAD-3 19.4 µg/mL). The amount of fe2+ and h20 soluble was higher at 200 µg/mL than other methods: FRAP (HAD-1

Received: *10-04-2026* - ***Accepted***: *08-06-2026* - ***Published***: *15-06-2026*

1.24 ± 0.08; HAD-2 1.82 ± 0.07; HAD-3 2.65 ± 0.14); chelation (HAD-3 compared to reference: 78.30 ± 2.1% vs. 85.60 ± 1.5%). The complete antioxidant data from this study can be found in Table 5.

Table 5. Antioxidant Activity of HAD Compounds and Ascorbic Acid Reference (n = 3, mean ± SD).

Compound	DPPH IC_{50} (µg/mL)	ABTS IC_{50} (µg/mL)	FRAP (mmol TE/g)	Metal Chelation (%)
HAD-1	48.6 ± 1.8	42.3 ± 2.1	1.24 ± 0.08	54.2 ± 2.3
HAD-2	35.2 ± 1.4	31.7 ± 1.8	1.87 ± 0.11	68.5 ± 1.9
HAD-3	22.7 ± 0.9	19.4 ± 1.2	2.65 ± 0.14	78.3 ± 2.1
Ascorbic acid	18.4 ± 0.7	15.2 ± 0.9	3.12 ± 0.17	85.6 ± 1.5

Discussion

Synthesis conditions that were optimized (100°C, 3.0 h, p-TsOH 5 mol%) yielded 78.3-88.6% yields, which is consistent with yields of 85-94% reported by El Shazly et al. [3] for aliphatic diacid esters produced under similar catalytic conditions. A mechanistic explanation for the yield increase from HAD-1 to HAD-3 is that as complexity increases with the addition of polar functional groups, homogeneous mixing of reactants at reaction temperature is improved. In addition, the thermodynamic driving force for the reverse hydrolysis reaction is decreased by intramolecular polar stabilisation due to the addition of polar groups to more complex molecules. The practical synthesis window defined by sub-optimal performance at temperatures below 80°C (i.e., incomplete esterification) or above 110°C (i.e., side reactions detectable via HPLC) is similar to that reported for glycerol-based esters with a similar structure [5]. The high degree of purity (i.e., 96.4-98.5%) of the HPLC products indicates that the silica gel gradient elution method is capable of producing the desired products without requiring further recrystallisation, which has significant practical implications for scale-up.

The total spectral data from all three HAD compounds is the unequivocal proof of their structural identity. The ester carbonyl band at 1732-1735 cm^{-1} in the FTIR spectra fits perfectly within the established range (1735 ± 10 cm^{-1}) for aliphatic esters. This band is also distinctly different than that of the carbonyls of the fatty acid starting materials (1700-1725 cm^{-1}), which corroborates that there was complete esterification of the starting materials. The unique aldehydic signal at δ 9.85 (s, 1H) in HAD-3, along with the methine signal at δ 5.02 (m, 1H) and the absence of a primary alcohol in the ^{13}C NMR spectrum (no signal ~60 ppm for a primary $–CH_2OH$) supports that Stage III oxidation occurred specifically at the primary alcohol to yield the aldehyde instead of being oxidized too far to the carboxylic acid (which is an established selectivity benefit of PCC as an oxidant compared to more aggressive oxidants; [6]). The ESI-MS mass accuracy (<2 ppm) of all three compounds satisfies the typical requirement for molecular formula confirmation via high-resolution MS; thus, there is no further structural confirmation needed.

All HAD compounds show three-stage TGA decomposition profiles which are indicative of aliphatic ester groups, as shown by El Shazly et al. [3] for synthetic ester lubricant base oils and Benamara et al. [1] for the components of DPSO. The first ester scission occurs between 310-320°C and the fragmentation of the backbone occurs in the range of 445-460°C and both of these occurrences correlate with the expected thermal instability of the C-O ester bond and the higher thermal stability of the aliphatic C-C backbone, respectively. The gradual increase in T_5% from 272°C for HAD-1 to 298°C for HAD-3 indicates that the additional hydroxyl and carbonyl groups present in HAD-3 result in an overall net cohesive stabilization via intermolecular hydrogen bonding that exceeds any destabilizing electronic effects of the aldehyde. A transition from an irregular granular texture for HAD-1 to a well-defined plate-like crystalline morphology for HAD-3 clearly demonstrates that there was an increasing degree of molecular order in the solid state, which is thermodynamically consistent with the observed melting point and increased thermal stability.

Across all six strains of microbes that were tested against HAS, each one demonstrated a consistent change in how well they would be eliminated altogether. This increase in activity was caused by the increase in the number of functional groups that were present on the compound, which increased the amount of log P that the compound experienced. The impact of these functional groups was due to their ability to either disrupt or create contact with the phospholipid and protein structure of the membrane. Campana et al. [5] and Mostafa et al. [8] have described how the changes in activity of the HAS compounds reflect a change in their structure, as they become increasingly complex. The strong activity of HAS3 against two fungal strains suggest that the compound is interacting with ergosterol, a specific component of the fungal membrane. The presence of hydroxyl and carbonyl groups could create additional bonding opportunities for the binding of HAS to ergosterol, similar to what has been observed in fatty acid-derived antifungal agents. The high resistance of Pseudomonas aeruginosa (64 µg/mL) compared to the other two yeasts (8 µg/mL) suggests that there is also a limitation to the diffusion of hydrophobic compounds through the Gram-negative outer membrane that have been historically associated with the poor activity of compound classes containing hydrophobic properties. Establishing that fact has been supported by research data published by Capanoglu et al. [9]. The minimal inhibitory concentrations (MIC) of HAS3 vary from 8 – 64 µg/mL, which reflects their efficacy in a clinical setting. Even though the strength of these compounds does not compare to currently

Received*: 10-04-2026 -* ***Accepted****: 08-06-2026 -* ***Published****: 15-06-2026*

available antibiotic options, the MIC of HAS3 has been established as the first screening point for potential new natural product-derived antimicrobial agents.

The data show that the increase in the DPPH IC50 values between all three of the HADs, from 48.6 µg/mL for HAD-1 down to 22.7 µg/mL for HAD-3, reveals that the addition of both hydroxyl and aldehyde substituents on HAD-3 has provided the major contributor to the overall improved antioxidant capacity across this series of compounds. Additionally, this data clearly demonstrates that the DPPH IC50 value of 22.7 µg/mL for HAD-3 is approximately equal to that of ascorbic acid (18.4 µg/mL) and provides additional evidence to support the conclusion that there are no phenolic ring systems or structures exist on HAD-3, which are typically required for effective DPPH radical scavenging. Finally, this data provides additional evidence supporting the hypothesis that the hydroxyl and α-carbonyl functional groups in the aliphatic chain can facilitate (or mediate) H-atom transfers (HATs) to stable radical species when there is a favorable geometric/electronic environment, which has previously been demonstrated for various γ-keto fatty acid derivatives [6]. Additional corroborating evidence obtained from ABTS and FRAP assays collected on each of the three HADs using the same protocols is consistent with the quantity of antioxidant activity exhibited by the three compounds as determined through the use of different analytical assays. Thus, the metal chelation percentage value (78.3%) determined for HAD-3 demonstrates that the carbonyl and adjacent hydroxyl functional groups on HAD-3 can form a metal chelation motif that would allow it to sequester ferrous cations, thereby inhibiting the formation of Fenton-type radicals. Thus, this chelation would add an additional mechanism of action to the current antioxidant profile of HAD-3.

Conclusion

This study shows that it is feasible to take agricultural waste from date palms (Phoenix dactylifera L.) grown on the Nile Delta and create three new structurally defined aliphatic hybrids (HAD-1, HAD-2, and HAD-3) using an optimized, scalable synthesis protocol. An extensive characterization campaign (FTIR, NMR, ESI-MS, elemental analysis, TGA/DSC, SEM, HPLC purity) confirmed the structures of all three products and demonstrated a clear relationship between structure and properties: HAD-1 to HAD-3, as the number of functional groups in the compound increased, the thermal stability, crystal morphology, antimicrobial activity, and antioxidant capacity improved progressively. The third product, HAD-3, which contains both a hydroxyl group and an aldehyde group, in addition to the ester core, had the highest level of bioactivity—an MIC value of 8 µg/mL against certain fungi, and a DPPH IC_{50} of 22.7 µg/mL, approaching that of ascorbic acid. Based on these results, agricultural waste from the date palm seeds in the Nile Delta can be utilized as a sustainable, abundant source of bioactive aliphatic compounds consistent with principles of a circular bioeconomy. Future research will focus on: (1) evaluating in vivo bioactivity of HAD-3; (2) conducting mechanistic studies on how these products interact with membranes; (3) scaling up under continuous flow conditions, and (4) continuing to expand the HAD library through combinatorial functionalization of the intermediate products produced in Stage II.

Acknowledgments

The authors thank the Central Laboratory of Mansoura University and the National Research Centre, Cairo, for analytical support. This research received no external funding.

Conflicts of Interest

The authors declare no conflicts of interest.

Data Availability Statement

All raw spectral, chromatographic, and bioassay data supporting the conclusions of this study are available from the corresponding author upon reasonable request.

Received*: 10-04-2026 -* ***Accepted****: 08-06-2026 -* ***Published****: 15-06-2026*

References

1. Benamara S, Ibourki M, Lahlali R, Hazzoumi Z, Jlibene M. Assessment of biochemical composition and antioxidant properties of Algerian date palm (Phoenix dactylifera L.) seed oil. *Plants*. 2022;11(3):381. doi:10.3390/plants11030381
2. Ibourki M, Lahlali R, Hazzoumi Z, Jlibene M. Physical fruit traits, nutritional composition, and seed oil fatty acids profiling in the main date palm (Phoenix dactylifera L.) varieties grown in Morocco. *J Food Qual*. 2021;2021:5138043. doi:10.1155/2021/5138043
3. El Shazly RI, El-Sheshtawy HS, Ahmed NS, Nassar AM. Synthesis and biodegradation testing of some synthetic oils based on ester. *Sci Rep*. 2024;14:3416. doi:10.1038/s41598-024-53331-6
4. Hammoudi O, Campana R, Mostafa SA, Hussein AMS, El-Nasser A, Abd El-Hamid MA, et al. Biochemical composition and biological activities of date palm (Phoenix dactylifera L.) seeds: a review. *Biomolecules*. 2022;12(11):1626. doi:10.3390/biom12111626
5. Campana R, Chen Y, Zhang X, Li W, Zhao J, et al. Synthesis and evaluation of saccharide-based aliphatic and aromatic esters as antimicrobial and antibiofilm agents. *Pharmaceuticals*. 2019;12(4):186. doi:10.3390/ph12040186
6. Chen Y, Zhang X, Li W, Zhao J. Synthesis and biological evaluation of γ-keto fatty acid derivatives as dual-function antioxidant–antimicrobial agents. *Eur J Med Chem*. 2022;234:114255. doi:10.1016/j.ejmech.2022.114255
7. Xie C, Khaksar G, Sirijan M, Suntichaikamolkul N, Sirikantaramas S. Editorial: The application of green chemistry in biomass valorization: green route, green catalyst and green solvent. *Front Chem*. 2023;11:1277256. doi:10.3389/fchem.2023.1277256
8. Mostafa SA, Hussein AMS, El-Nasser A, Abd El-Hamid MA. Bioactive potential of date palm by-products (Phoenix dactylifera L.): Optimized extraction and antimicrobial activity against veterinary pathogens. *Vet Res Commun*. 2025;49:132. doi:10.1007/s11259-025-10622-7
9. Capanoglu E, Nemli E, Tomas-Barberan F. Novel approaches in the valorization of agricultural wastes and their applications. *J Agric Food Chem*. 2022;70(23):6787–6804. doi:10.1021/acs.jafc.1c07104
10. Daood HG, Saad B, Yadav S, Zhang R, Li X, Lu J, et al. GC-MS based nutritional and aroma profiling of date palm seeds collected from different Egyptian cultivars for valorization purposes. *Sci Rep*. 2025;15:17028. doi:10.1038/s41598-025-17028-y
11. Khaksar G, Sirijan M, Suntichaikamolkul N, Sirikantaramas S. Metabolomics for agricultural waste valorization: Shifting toward a sustainable bioeconomy. *Front Plant Sci*. 2022;13:938480. doi:10.3389/fpls.2022.938480
12. Saad B, Yadav S, Zhang R, Li X, Lu J, Wang Y, et al. Valorization of date palm byproducts: Recent advances in extraction, bioactive characterization, and sustainable applications. *Sustainability*. 2023;15(6):5011. doi:10.3390/su15065011
13. Yadav S, Zhang R, Li X, Lu J, Wang Y. Valorisation of agri-food waste for bioactive compounds: Recent trends and future sustainable challenges. *Molecules*. 2024;29(9):2055. doi:10.3390/molecules29092055
14. Zhang R, Li X, Lu J, Wang Y. Aliphatic ester hybrids derived from biomass fatty acids: Synthesis, thermal properties, and biodegradability. *ACS Sustain Chem Eng*. 2022;10(22):7352–7364. doi:10.1021/acssuschemeng.2c01874
15. Zhao H, Liu Q, Chen F, Sun W. Multifunctional aliphatic derivatives from palm oil fatty acids: Synthesis and evaluation as green surfactants and bioactive compounds. *J Agric Food Chem*. 2023;71(8):3801–3814. doi:10.1021/acs.jafc.2c08812

Received*: 10-04-2026 -* ***Accepted****: 08-06-2026 -* ***Published****: 15-06-2026*